Pergamon

Ann. Nucl. Energy, Vol. 24, No. 6, pp. 423–438, 1997

PII:S0306-4549(96)00026-6
0306-4549/97 $17.00 + 0.00

BUBBLE–BUBBLE INTERACTION FOR LAGRANGIAN TREATMENT OF MULTI-COMPONENT FLOW

RIZWAN-UDDIN[†‡]

Department of Nuclear Engineering, University of Illinois, Urbana, IL 61801, U.S.A.

(Received 4 March 1996)

Abstract—Interaction between bubbles for the simple case of a small spherical bubble in the vicinity of a much larger bubble—both rising in stationary liquid—with no mass transfer between liquid and vapor phases, has been studied numerically. The effect of the motion of the larger bubble on the dynamics of the smaller bubble has been determined both for completely spherical, and for spherical cap shaped large bubbles. The complicated motion of the smaller bubble, as it is entrained in the wake of the larger bubble, is clearly seen. This simple model of bubble–bubble interaction—that predicts the essential features observed in experiment—can be used in the computer simulation of individual-particle-tracking method (Lagrangian approach) of two-phase flow analysis. © 1997 Elsevier Science Ltd. All rights reserved.

NOMENCLATURE

A = cross sectional area of the bubble perpendicular to flow direction
C = drag coefficient
F_b = buoyancy force
F_d = drag force
R = radius
U = velocity
a = constants
g = gravity
r = distance of the smaller bubble from the larger bubble's center
u = velocity
x = x-location of the smaller bubble in absolute frame
y = y-location of the smaller bubble in absolute frame
α = angle
ρ = density
μ = viscosity

[†]Also Computational Science and Engineering Program.
[‡]Work performed while at University of Virginia.

Subscripts
b = bubble
d = drag
l = liquid
v = vapor
1 = larger bubble
2 = smaller bubble

INTRODUCTION

With larger and faster computers becoming more easily accessible, multi-phase flow analysis via modeling of each individual particle of the discrete phase, its motion, and interaction with other particles and container walls is becoming feasible. In fact, combined Eularian–Lagrangian approaches to model the continuous (liquid) and discrete (bubbles) phases have already been reported by Stuhmiller *et al.* (1989) and Trap *et al.* (1991). Modeling the interfacial phenomena accurately is one of the many difficult aspects of such individual-bubble-tracking Eularian–Lagrangian approaches. This includes the determination of bubble motion in the presence of other bubbles in the surrounding, development of interaction schemes between bubbles and surrounding walls, and development of interaction schemes among individual bubbles as they come close and pass each other or coalesce to form larger bubbles. Although it is necessary that the bubble dynamics models and interaction schemes are systematically developed using first principles, any interaction scheme based on first principles is likely to be complicated, or at least computer intensive in application, for problems of practical use. Hence, simpler interaction schemes based on phenomenological arguments must also be developed to be used in large scale individual-bubble-tracking computer simulations. These models must be validated against results from models based on first principles and against experimentally obtained data for single, few, and many bubbles rising and interacting in a liquid column.

Determination of the interaction models among multiple bubbles of various sizes is a very complicated problem (Lin *et al.* 1970; Wacholder and Sather, 1974), and can only be approached in a step by step fashion. An excellent review of the theoretical results for the motion of *solid* spherical particles in viscous fluid is given by Feuillebois (1989). Conditions under which these results are applicable to spherical *bubbles* are also discussed.

The goal of this overall exercise is not to develop a first-principle based interaction scheme between bubbles, which may take minutes (if not hours) of *CPU* time on reasonably large size work stations for a single interaction, but rather to have a simple model that can be repeatedly solved within reasonable cpu time for the hundreds or thousands of interactions that typically occur in multi-component flow, making it possible to be included in computer codes that are based on the Eularian–Lagrangian approach to multi-component flow. As a first step (proof-of-principle) toward the development of the interaction schemes, we have carried out analysis of bubble–bubble interaction for the simple case of the motion of a small bubble in the vicinity of a much larger vertically rising bubble in stationary liquid with no mass transfer between liquid and vapor phases. Though the analysis—which has been carried out for different shapes of the larger bubble including spherical bubble with no wake, spherical bubbles with wake and

spherical cap bubble—does not address the much more difficult question of whether coalescence occurs or not, it does correctly predict the essential features in bubble–bubble interactions observed in experiments, namely the wake effect, viscosity effect, etc. Some of these features are briefly discussed at the end of the next section.

BACKGROUND

A brief background of the dynamics of single bubble is first given. Laws and models for single bubble behavior in liquid column will be utilized in the next section in two ways: first to determine the terminal velocity of the larger bubble, and second, to determine the drag forces acting on the smaller bubble due to the velocity field generated by the moving larger bubble. Excellent reviews of this background information is given by Clift *et al.* (1978), O'Neill (1981), and Khan and Richardson (1987).

The equations of viscous motion with no-slip boundary condition were solved by Stokes (1851), who derived the expression, now known as Stokes law, for the terminal velocity of a *rigid* spherical particle in fluid of infinite extent,

$$u_\infty = \frac{2g\,(\rho_l - \rho_v) r_b^2}{9\mu} \tag{1}$$

where u_∞ is the steady-state terminal rise velocity, ρ is density, r is radius, μ is viscosity, g is gravity and subscripts l, v and b represent liquid, vapor and bubble, respectively. The corresponding expression for the terminal rise velocity of a *bubble* in fluid of infinite extent is given by Levich (1949,1962),

$$u_\infty = \frac{g\,(\rho_l - \rho_v) r_b^2}{9\mu}\,. \tag{2}$$

Expressions for the drag force exerted by the fluid on the particle are also well known. The difficulties encountered in extending the above results analytically to more general and realistic cases with non-rigid and non-spherical shaped bubbles, led to the introduction and wide spread use of the drag coefficient, defined by the equation

$$F_d = \frac{C_d\,\rho_l u^2 A}{2g}$$

where F_d is the drag force on the particle, C_d is the (dimensionless) drag coefficient, A is the cross-sectional area of the particle perpendicular to the direction of flow and u is the particle velocity relative to the liquid phase. Though there were exceptions (Moore, 1959, 1963; Hartunian and Sears, 1957; Walters and Davidson, 1962), most of the early works on the dynamics of bubble motion in liquid were carried out experimentally (O'Brien and Gosline, 1935; Pebbles and Garber, 1958; Uno and Kintner, 1956; Harmathy, 1960). Among other findings these studies determined the range of Reynolds number for the validity of Stokes law applied to gas bubbles in liquids, and experimentally showed that Stokes law, which also can be written as a function of Reynolds number Re, as,

$$C_d = \frac{24}{\mathrm{Re}} \quad \text{where} \quad \mathrm{Re} \equiv \frac{2r_b u \rho_l}{\mu},$$

agrees well with data for Re < 2. For other ranges of Reynolds number and other dimensionless parameters, correlations for the drag coefficient also were experimentally obtained, e.g. for 2 < Re < 200 it was found by Allen (1900) that,

$$C_d = \frac{18.5}{\mathrm{Re}^{0.6}}.$$

An important factor for the significant functional changes in the drag coefficient's dependence on Reynolds number is that the shape of the rising bubble changes considerably as Reynolds number increases. For air bubbles in water, four general categories of bubble shapes were experimentally determined by Robinson (1947),

(a) Spherical bubbles,	Re < 400
(b) Oblate spheroids of varying geometric proportion	400 < Re < 1100
(c) Oblate spheroids of constant geometric proportions	1100 < Re < 5000
(d) Mushroom shaped bubbles with spherical cap	5000 < Re.

More recently, Narayanan *et al.* (1974) also have given a similar classification.

Spherical cap bubbles are usually described by the radius of curvature and the angle α, defined by drawing normals to the cap of the spheres, as shown in Fig. 1. Rippin and Davidson (1967) showed, using inviscid flow theory, that α approaches approx. 100° for high Reynolds number and this has been confirmed experimentally for Re $\gtrsim$ 100 by Grace (1970). For intermediate Reynolds number (5 < Re < 100), the relation between α and Re is given by Davidson *et al.* (1977),

$$\mathrm{Re} = 8 \left\{ \frac{4}{2 - 3\cos\left(\frac{\alpha}{2}\right) + \cos^3(\alpha/2)} \right\}^{2/3}.$$

For mushroom shaped large air bubbles, terminal velocity was experimentally determined and was found to be independent of liquid properties for the two liquids used in experiment, water and nitrobenzene. Terminal velocity was related to the radius of curvature of the spherical cap r, by Davies and Taylor (1950)

$$U_\infty = 0.667\sqrt{gr} \tag{3}$$

and radius of curvature r and equivalent spherical radius based on vapor volume were found to be related by,

$$r = 2.3r_b \tag{4}$$

Though an expression for the terminal rise velocity of an ellipsoidal cap bubble with an eccentricity e has been derived by Wairegi and Grace (1976), it has been reported by Bhaga and Weber (1981) that Davies and Taylor's (1950) expression for terminal rise velocity agreed with their data within 5% for $R > 10$ if the radius was obtained by fitting a sphere over the front 75° segment. Detailed structure of the wake behind rising bubbles also has been investigated by several investigators including Narayanan *et al.* (1974), Komasawa *et al.* (1980), Bhaga and Weber (1980, 1981).

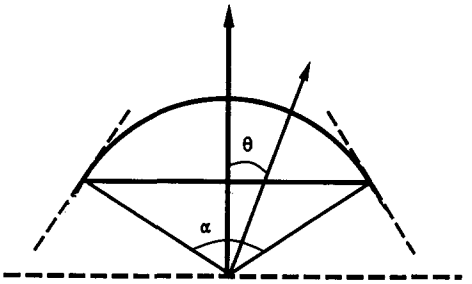

Fig. 1. Schematic diagram of a spherical cap bubble and the definition of the angle α defined by drawing normals to the cap of the sphere.

Studies on the motion of a stream of air bubbles rising in a liquid column have been carried out experimentally by O'Brien and Gosline (1935), van Krevelen and Hoftijzer (1951), and others to determine the mean rise velocity as a function of gas flow rate, without measuring the bubble sizes. Data was, in general, used to develop correlations relating such desired quantities as rise velocity with dimensionless numbers of the system. The effect on the dynamics of a bubble of the motion of another bubble in the neighborhood has been studied experimentally in the context of coalescence and breakup of bubbles in liquids by Crabtree and Bridgewater (1971), Narayanan *et al.* (1974), Otake *et al.* (1977), Bhaga and Weber (1980) and Stewart (1995). It was observed that the leading bubble, due to the wake effect, induced an increment in the rise velocity of the following bubble, hence, making coalescence more probable. Due to the poor understanding of the complex wake structure behind bubbles, which is necessary for analytical analysis of bubble–bubble interaction, attempts toward the development of models—to be used in the numerical simulation analysis of two-phase flow by following the dynamics of each individual bubble in a continuum of liquid—to describe the interaction of two or more nearby bubbles, have been limited. Experiments conducted in liquid columns and fluidized beds show that the fluid, as visualized using tracers by Weber and Bhaga (1982) or a smaller bubble, in the path of a larger (rising) bubble actually moves side ways as the larger bubble nears it, and the tracer or small bubbles may actually get entrained in the wake behind the larger bubble, and in the case of bubbles speed up and coalesce with the larger bubble. The latter part of this scenario is similar to experimental observations by de Nevers and Wu (1971), Narayanan *et al.* (1971), and Bhaga and Weber (1980), that each bubble trails a wake, and that the bubble that coalesces from below actually accelerates as it enters the wake of the preceding bubble and hence attempts to overtake the first bubble. de Nevers and Wu (1971) also found that the predictions of their detailed model were not significantly altered by different assumed wake configurations.

MODEL

The larger bubble being more buoyant moves faster than the leading smaller bubble and hence, depending upon the values of various parameters and initial conditions, overtakes the smaller bubble, which then either coalesces with the larger bubble or falls behind. Of course, we assume the liquid is otherwise stationary, and the smaller bubble

is initially ahead of the larger bubble close to the vertical line passing through the centre of the larger bubble. The motion of the larger trailing bubble, we assume, is not affected as it approaches the much smaller leading bubble and hence the large bubble keeps moving vertically up in a straight line with its terminal velocity, given by equation (2) or equation (3), depending upon bubble shape. Unless there is contact between bubbles, motion of one bubble affects the dynamics of the surrounding bubbles through the displacement of the liquid that fills the space between them, i.e. by the velocity field created by their motions. The velocity field, due to the assumption of one bubble being much larger than the second bubble, is essentially that developed due to the motion of the larger bubble. Hence, the smaller bubble, which quickly reaches steady-state and rises with uniform terminal velocity in the absence of the larger bubble, is affected by the velocity field generated by the motion of the larger bubble. As the distance between the larger and smaller bubbles decreases, the fluid that is displaced by the motion of the larger bubble exerts a drag force on the smaller bubble. The dynamics of the smaller bubble, using symmetry around the vertical axis, is determined in a vertical plane that passes through the centers of both bubbles, by solving the bubble dynamics equations in x and y directions obtained by equating the net force acting in each direction to mass times the acceleration in that direction,

$$m_b \ddot{x} = - F_d^x \tag{5}$$

$$m_b \ddot{y} = - F_d^y + F_b \tag{6}$$

where m_b is the effective mass of the bubble, F_d is the drag force, F_b is the buoyancy force, and x and y are the coordinates of the smaller bubble in the stationary frame, see Fig. 2. The drag forces in the x and y directions are respectively proportional to the difference in the bubble velocity and velocity of the surrounding fluid—that is generated

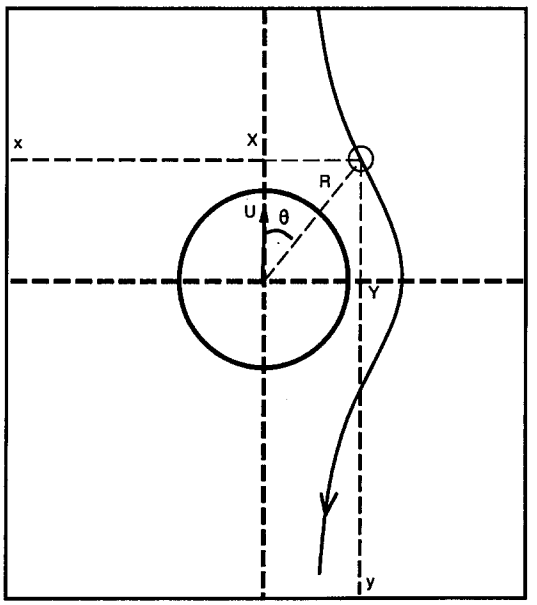

Fig. 2. Schematic diagram of a large and a small bubble, and the definition of X, Y, R and θ.

due to the motion of the larger bubble in the vicinity—in the x and y directions, and are given by Lamb (1945),

$$F_d^x = 12\,\pi\,\mu\,r_2\,(u_1 - \dot{x}) \tag{7}$$

$$F_d^y = 12\,\pi\,\mu\,r_2\,(v_1 - \dot{y}) \tag{8}$$

where r_2 is the radius of the smaller bubble and, $u_1\,(x,y)$ and $v_1\,(x,y)$ are the liquid velocity induced by the larger bubble in the stationary frame, in the x and y directions, respectively. Note that the drag force on bubbles, as shown by Levich (1962), is twice as much as on solid spherical bodies.

To solve equations (5) and (6) for the motion of the smaller bubble, one must know the velocity field (u_1,v_1). Models for fluid motion around spheres and around spherical caps have been developed in the past. We use these models, described below, to determine the liquid velocity induced by the motion of the larger bubble at the site of the smaller bubble and solve equations (5) and (6) with appropriate initial conditions to determine the dynamics of the smaller bubble. Since bubbles of large volume do not retain complete spherical shape, the dynamics of smaller bubbles has been determined both for large complete spherical bubbles and for spherical cap shaped large bubbles.

Large spherical bubble with no wake

When the fluid motion induced by a moving sphere is determined using non-viscous flow conditions with zero fluid velocity at a distance from the sphere, the resulting flow, symmetric around the axis of bubble motion, is given by the stream function (Batchelor, 1967).

$$\psi = -\frac{1}{2}\,U\,\frac{r_1^3}{R^2}\sin^2\theta \tag{9}$$

or in terms of the velocity potential ϕ, by

$$\phi = -\frac{1}{2}\,U\,r_1^3\,\frac{\cos\theta}{R^2}$$

where r_1 is the bubble radius, U is the bubble velocity and R and θ are explained in Fig. 2. Hence, the fluid velocity, as observed by a stationary observer, is given by

$$u_1 = -\frac{1}{Y}\frac{\partial\psi}{\partial Y} = \frac{U_1}{2}\left(\frac{r_1}{R}\right)^3\{1 - 3\cos^2\theta\} \tag{10}$$

$$v_1 = -\frac{1}{Y}\frac{\partial\psi}{\partial X} = -\frac{3}{2}\,U_1\sin\theta\cos\theta\,\left(\frac{r_1}{R}\right)^3. \tag{11}$$

However, if the fluid motion induced by the moving sphere is determined using no-slip boundary condition at the sphere surface, for small Reynolds number, Re, by ignoring the inertia forces, it is given by the stream function (Lamb, 1945),

$$\psi = \frac{3}{4} U r_1 R \left(1 - \frac{1}{3}\frac{r_1^2}{R^2}\right) \sin^2 \theta. \tag{12}$$

The fluid velocity, as observed by a stationary observer, in this case becomes

$$u_1 = U\left(\frac{r_1}{R}\right)\left\{1 + \frac{1}{2}\left[1 - \left(\frac{r_1}{R}\right)^2\right]\left[1 - \frac{3}{2}\sin^2\theta\right]\right\} \tag{13}$$

$$v_1 = \frac{3}{4} U r_1 \frac{\sin\theta\cos\theta}{R}\left[1 - \left(\frac{r_1}{R}\right)^2\right]. \tag{14}$$

Using the liquid velocities induced by the larger bubble given above, equations (10) and (11) or equations (13) and (14), the dynamics of the smaller bubble in the vicinity of the larger bubble can be solved using equations (5) and (6). Since the vortex and the wake effect behind the larger bubble is not explicitly included, these models do not include the pulling force exerted by the larger bubble on the smaller bubble in its wake which contributes to coalescence.

Large spherical bubble with wake

As discussed earlier, the wake effect plays an important role in determining bubble dynamics, and that entrainment in the wake of a leading bubble is considered to be the prime mechanism for bubble coalescence. Though it is known that in laminar flow the width of the wake and liquid velocity decrease with distance, the wake structure behind bubbles is poorly understood as any attempt to measure velocities in the wake also affects the bubble motion. See Fig. 3. We assume that the vertical velocity in the wake can be written as (Stuhmiller *et al.* 1989).

$$U_{\text{wake}}(\xi,\eta) = U_{\text{d}}(\xi)\, e^{-a_1\left(\frac{\eta}{\eta^*(\xi)}\right)^2} \tag{15}$$

where ξ is the distance from the bubble center, η is the perpendicular distance form the line passing through the bubble center, and η^* scales the velocity at different ξ values, and is assumed to be given by

$$*(\xi) = a_2 e^{-a_3 \xi}, \tag{16}$$

which results in exponentially decreasing wake width behind the bubble. The center line velocity in the wake behind the bubble $U_d(\xi)$ is also assumed to decrease exponentially

$$U_{\text{d}}(\xi) = U_0\, e^{-a_4\left(\frac{\xi}{r_1} - 1\right)}, \tag{17}$$

where r_1 is the bubble's radius, U_o is bubble's velocity, and a_i (i= 1,2,3,4) are constants. Note that this choice of U_{wake} (ξ,η), for a given ξ, results in a Gaussian distribution of velocity in η, where both the peak and spread of the Gaussian decrease

exponentially with ξ. Also note that the wake velocity calculated using equation (15) is actually super imposed on velocity given by equations (10) and (11) or equations (13) and (14).

Large spherical cap bubble with wake

It is well known that large bubbles assume the shape of a spherical cap (Parlange, 1969; Wegener and Parlange, 1973). This permits a recirculating flow region underneath the spherical cap that is larger than the corresponding region for a spherical bubble of the same radius. In the case of the larger vapor bubble of spherical cap shape, we assume the bubble is followed by a Hills vortex and hence, the flow inside a closed region right under the spherical cap is given by the stream function (Lamb, 1945)

$$\psi = -\frac{3}{4} UR^2 \sin^2\theta \left(1 - \left(\frac{R}{r_1}\right)^2\right) + \frac{1}{2} UR^2 \sin^2\theta$$

where the bubble induced velocity outside the vortex is given by equations (10) and (11).

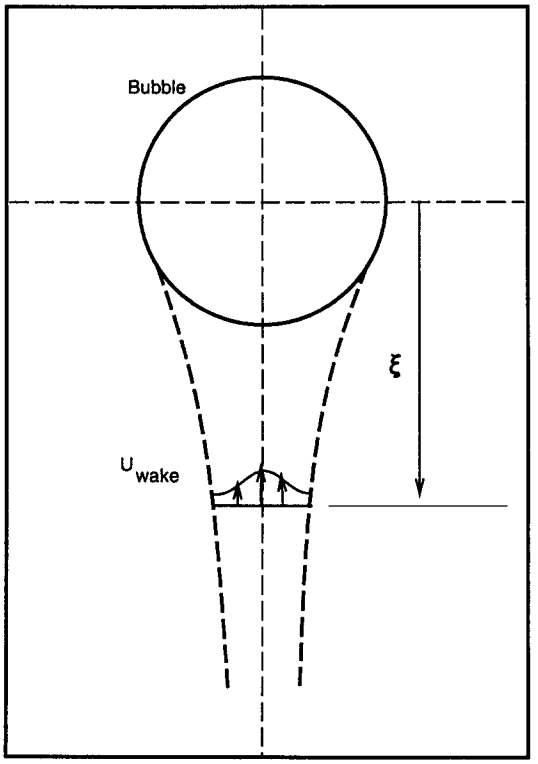

Fig. 3. Schematic diagram of the wake behind a bubble. For laminar flow, the width of the wake and the velocity at the center line are assumed to decrease exponentially with distance from the vertical line passing through the bubble's center.

RESULTS AND DISCUSSION

The models for velocity fields generated by different bubble shapes and different assumption, described in the section above, were used to simulate the fluid motion induced by the rising motion of a bubble. The motion of a small spherical bubble along the path (in the vicinity) of the larger bubble was then determined by solving equations (5) and (6). Simple fourth order Runge–Kutta scheme was used to numerically integrate equations (5) and (6). In all the results reported below, though the larger bubble is at rest at $t = 0$, it reaches its terminal velocity on a time scale much shorter than the time scale for the interaction between smaller and larger bubble. By choosing the vertical distance between the two bubbles at $t = 0$ to be large enough we ensure that there is no interaction between the bubbles before the larger bubble reaches its terminal velocity.

Results of a typical analysis of the motion of the smaller bubble of 1 mm radius, initially 2 mm from the vertical line passing through the center of the larger bubble, is shown in Fig. 4. Larger bubble's radius is 5 mm. Shown in Fig. 4(a) is the motion of the smaller bubble in coordinate axes fixed at the center of the (moving) larger bubble. Figure 4(b) shows the vertical location of both bubbles as a function of time. The fact that the smaller bubble is treated as a point particle allows it to come that close to the surface of the larger bubble, and it is unlikely that the two bubbles would actually touch when the center of the smaller bubble appears to be touching the surface of the larger bubble.

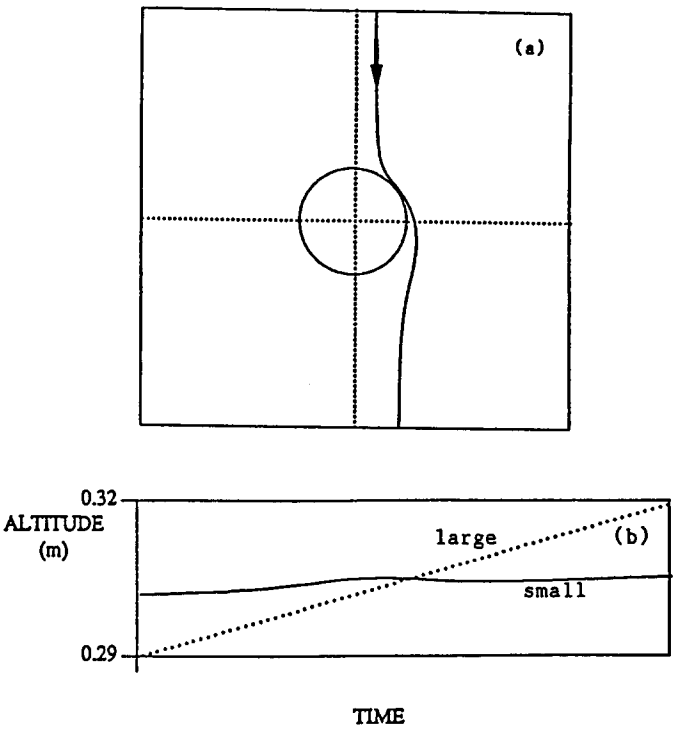

Fig. 4. A typical path of the smaller bubble as the larger bubble passes by it. (a) In the frame fixed at the center of the larger bubble; (b) in laboratory frame (the vertical location of the two bubbles as a function of time).

The effect of various parameters like bubble radii, liquid viscosity, and various initial conditions were numerically studied for the different models. This is reported first for the case when induced fluid motion is determined using non-viscous flow conditions [equations (10) and (11)] and when there is no wake behind the larger bubble. Results of all subsequent calculations (Figs 5–11) are reported in the frame fixed at the center of the larger bubble.

Figure 5 shows the motion of the smaller bubble, with respect to the larger bubble, for different initial conditions. As expected, the effect of the larger bubble on the motion of the smaller one significantly decreases if the smaller bubble is initially farther away from the vertical line passing through the larger bubble. Once again, since the smaller bubble is treated as a point particle, in two cases it appears to touch the larger bubble. The effect of viscosity of the liquid on the bubble–bubble interaction is shown in Fig. 6.

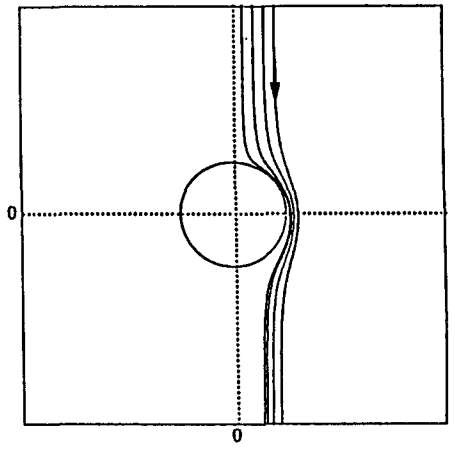

Fig. 5. The effect of horizontal distance between the two bubbles on the dynamics of the smaller bubble for induced flow calculated assuming non-viscous flow conditions. Shown are four paths of the smaller bubble starting from initial conditions at 1, 2, 3 and 4 mm from the vertical line passing through the center of the larger bubble.

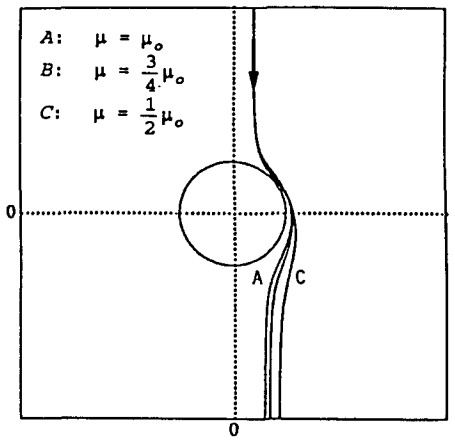

Fig. 6. The effect of viscosity on the dynamics of the smaller bubble.

An increase in viscosity (by a factor of two) results in an increased drag force and hence, the smaller bubble more closely follows the streamlines generated due to the motion of the larger bubble. The effect of the radius of the larger bubble also was studied. Note that the analysis is valid only for cases where $r_1 \gg r_2$, so that the smaller bubble does not influence the motion of the larger bubble. Figure 7 shows bubble motion for two larger bubbles of different radii, 5 mm and 7.5 mm. The smaller bubble initially is at a distance of 2 mm from the vertical line in both cases.

The above simulations were next repeated for case II in which the larger bubble induced fluid motion is determined by using the no-slip boundary condition, equations (13) and (14). Although more appropriate for solid spheres, it has been suggested that due to the contamination in the liquid—which leads to friction on the bubble surface—

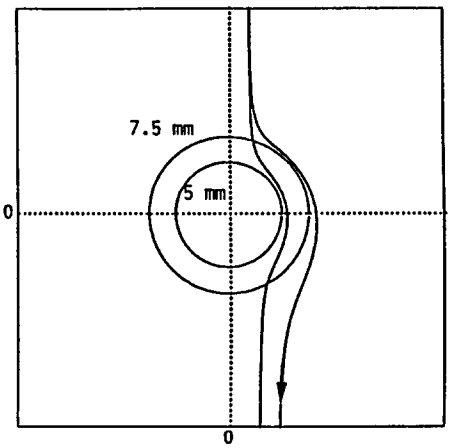

Fig. 7. The effect of larger bubble's diameter on the dynamics of the smaller bubble. In both cases, the initial horizontal distance between the two bubbles is 2 mm.

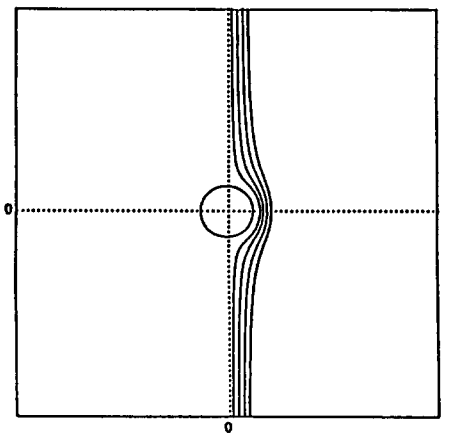

Fig. 8. The effect of initial conditions on the dynamics of the smaller bubble for induced flow calculated using no-slip boundary condition (Stokes solution). Shown are four paths of the smaller bubble starting from initial conditions at 1, 2, 3 and 4 mm from the vertical line passing through the center of the larger bubble.

this boundary condition also is relevant for bubble induced flow (Batchelor, 1967). The effect of different initial conditions on bubble dynamics is shown in Fig. 8. A comparison with Fig. 5 shows that in this case bubbles follow the streamlines more closely due to the higher drag force. The drag force, due to high viscosity—necessary because the analysis is valid only for small Reynolds number—is so high that a small change in viscosity does not significantly effect the path of the bubbles. The effect of the size of the larger bubble is shown in Fig. 9. Shown are the paths of the smaller bubble, initially 2 mm away from the vertical line passing through the larger bubble, for larger bubble of 5 and 7.5 mm radius.

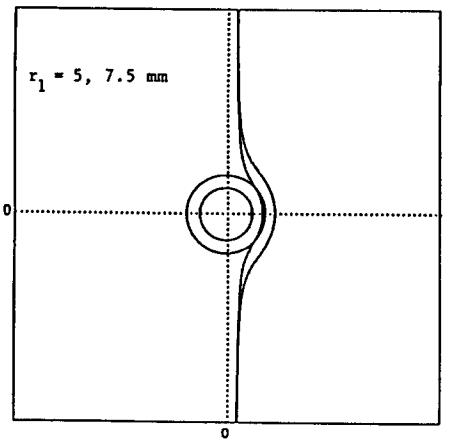

Fig. 9. The effect on the dynamics of the smaller bubble of the larger bubble's diameter for Stokes flow around the larger bubble.

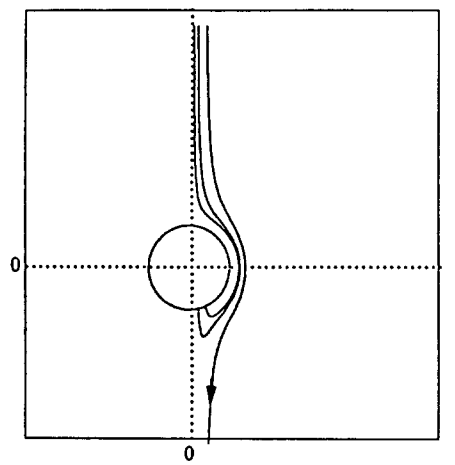

Fig. 10. The effect of horizontal distance between the two bubbles when the vertical velocity due to the wake effect behind the larger bubble also is included. Shown are three trajectories of the smaller bubble with initial horizontal distance between the center of the smaller bubble and the vertical line passing through the center of the larger bubble equal to 0.5, 1 and 2 mm. The smaller bubble gets trapped in the wake (as shown in Fig. 3) when its initial horizontal distance from the larger bubble is 0.5 or 1 mm. The larger bubble's radius is 5 mm.

The dynamics of the smaller bubble was next studied by introducing the wake effect and adding the vertical velocity in the wake, as determined by equation (15), to the liquid velocity field determined by equations (10) and (11). For a spherical larger bubble, results for the case of the smaller bubble starting from three different initial conditions (0.5, 1 and 2 mm away from the line passing through the center of the larger bubble) are shown in Fig. 10. For the first two initial conditions, the smaller bubble gets entrained in the wake and as a result eventually *hits* the larger bubble which may result in coalescence. This is very similar to bubble coalescence behavior observed in experiments reported by Davidson and Harrison (1971). For the third initial condition, since the smaller bubble is initially sufficiently removed from the larger bubble, it escapes the wake behind the larger bubble.

For the case of the spherical cap large bubbles, the fluid motion outside the vortex is the same as that given by case (I) and the motion inside the vortex is assumed to be given by Hills vortex. For large viscosity fluids, bubbles trapped in the vortex closely follow the circulatory motion in the Hills vortex and, due to the large drag forces, remain trapped. In other cases the smaller bubble leaves the vortex as the larger bubble speeds away, or it may merge with the spherical cap bubble. Since the current model cannot move a small bubble from outside the vortex to inside the vortex, the dynamics induced by the vortex motion is studied by assuming initial conditions for the smaller bubble inside the vortex. In practice it is expected that noise in the system would *push* some of the smaller particles in the vortex region. Shown in Fig. 11 are two cases of smaller bubble trapped in the vortex (initial conditions inside the vortex). For the case of large liquid viscosity, the bubble while slowly drifting out, follows the circulatory motion of Hills vortex, and in the process gets trapped at a location at the bottom of the vortex with zero velocity in the horizontal direction and vertical velocity exactly equal to the larger bubbles' rise velocity. The drag force at this point, due to the relative motion of the smaller bubble and vortex flow, exactly cancels the buoyancy force, and hence, at least theoretically, the smaller bubble keeps following the larger bubble with a constant

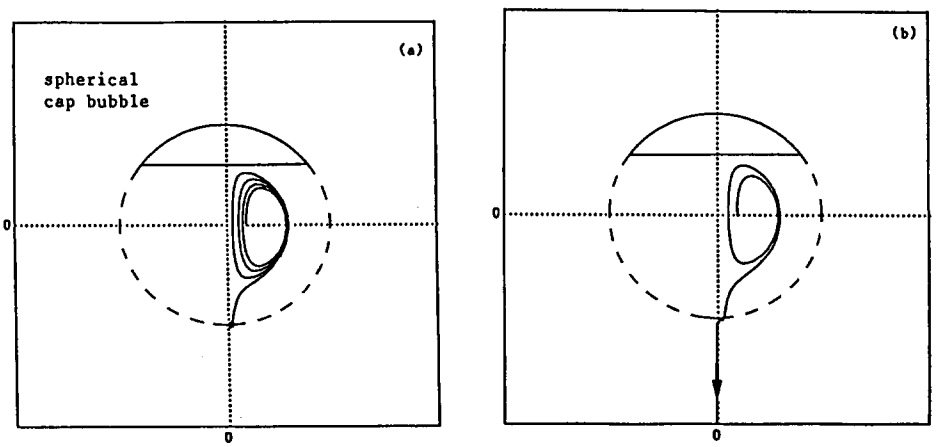

Fig. 11. The dynamics of a small bubble inside a Hills vortex behind a rising spherical cap bubble. Figure 11(a) shows the case when the smaller bubble gets trapped in the Hills vortex and moves with the larger bubble. As the viscosity is decreased, the smaller bubble, as shown in Fig. 11(b) is able to escape from the vortex.

distance between them, Fig. 11(*a*). This behavior is not observed as the viscosity of the fluid is decreased, and as shown in Fig. 11(*b*), at lower viscosities the smaller bubble is able to *escape* from the Hills vortex as the larger bubble speeds away. Once again, due to noise sent in the system, in practice we do not expect the small bubble—for high viscosity case—to be completely stationary (in the frame moving with the larger bubble). Instead it will most likely *dance around*, and may even jump out of the trapping region to either return back to the vortex or to escape the vortex entirely.

Results of the simulations clearly show that the simple model described here is capable of capturing the essential features of interaction between a large and a small bubble, and can be used in large scale simulations of multi-component flow using combined Eularian–Lagrangian approach.

SUMMARY

Due to increased emphasis on two-phase flow simulations using combined Eularian–Lagrangian approach (by following the dynamics of individual particles of the discrete phase), we have developed models to study the dynamics of small bubbles in the vicinity of large spherical bubbles with and without vortex and in the vicinity of mushroom type spherical cap bubbles. The effects of various physical parameters have been studied and it is found that the numerical analysis in the case of a spherical cap bubble predicts a point behind the large bubble where a small bubble can get trapped and follow the large bubble with zero relative velocity. This behavior is not observed at lower viscosities. Simple model described here can be very useful in analysing multi-component flow using combined Eularian–Lagrangian approach.

REFERENCES

Allen, H. S. (1900) *Phil. Mag.* **50**, 323.
Batchelor, G. K. (1967) *An Introduction to Fluid Dynamics.* Cambridge Univ. Press, Cambridge.
Bhaga, D. and Weber, M. E. (1980) *Chem. Eng. Sci.* **35**, 2467.
Bhaga, D. and Weber, M. E. (1981) *J. Fluid Mech.* **105**, 61.
Crabtree, J. R. and Bridgewater, J. (1971) *Chem. Eng. Sci.* **26**, 839.
Davidson, J. F. and Harrison, D. (Eds.) (1971) *Fluidization.* Academic Press, New York.
Davidson, J. F., Harrison, D., Darton, R. C. and LaNauze, R. D. (1977) In *Chemical Reactor Theory. A Review*, eds L. Lapidus and N. R. Amundson), Chap. 10. Prentice Hall, Englewood Cliffs, NJ.
Davies, R. M. and Taylor, G. (1950) *Proc. Roy. Soc., Ser. A.* **200**, 375.
de Nevers, N. and Wu, J-L. (1971) *AIChE J.* **17**, 182.
Feuillebois, F., (1989) In *Multiphase Science and Technology*, eds G. F. Hewitt, J. M. Delhaye and N. Zuber, Vol. 4. Hemisphere Publishing Corporation, New York.
Grace, J. R. (1970) *Can. J. Chem. Eng.* **48,** 30.
Harmathy, T. Z. (1960) *AIChE J.*, **6**, 281.
Hartunian, R. A. and Sears, W. R. (1957) *J. Fluid Mech.* **3**, 27.
Komasawa, I., Otake, T. and Kamojima, M. (1980) *J. Chem. Eng. Jap.* **13**, 103.

Lamb, H. (1945) *Hydrodynamics.* Dover Publications, New York.
Levich, V. G. (1949) *Zh. Eksp. Teoret. Fiz.* **19**, 18.
Levich, V. G. (1962) *Physiochemical Hydrodynamics.* Prentice Hall, Englewood Cliffs, NJ.
Lin, C. J., Lee, K. J. and Sather, N. F.(1970) *J. Fluid Mech.* **43**, 35.
Moore, D. W. (1959) *J. Fluid Mech.* **6**, 113.
Moore, D. W. (1963) *J. Fluid Mech.* **16**, 161.
Narayanan, S., Goosens, L. H. J. and Kossen, N. W. F. (1974) *Chem. Eng. Sci.* **29**, 2071.
O'Brien, M. P. and Gosline, J. E. (1935) *Ind. Eng. Chem.* **27**, 1436.
Otake, T., Tone, S., Nakoe, K. and Mitsuhashi, Y. (1977) *Chem. Eng. Sci.* **32**, 377.
Parlange, J-Y. (1969) *J. Fluid Mech.* **37**, 257.
Pebbles, F. N and Garber, H. J. (1958) *Chem. Eng. Prog.* **49**, 88.
Rippin, D. W. T. and Davidson, J. F. (1967) *Chem. Eng Sci.* **22**, 217.
Robinson, J. V. (1947) *J. Phys. Coloid. Chem.* **51**, 431.
Stewart, C. W. (1995) *Int. J. Multiphase Flow* **21**, 1037.
Stokes, G. G. (1851) *Trans. Camb. Phil. Soc.* **9**, 8.
Stuhmiller, J. H., Ferguson, R. E. and Meiser, C. A. (1989) Final Report EPRI NP-6557.
Trapp, J. A., Mortensen, G. A. and Ransom, V. H. (1991) In *Adv. in Math., Comp., and Reactor Phys.*, Vol. 1, 3.1 3-1–3.13-12. Am. Nuc. Soc.
Uno, S. and Kintner, R. C. (1956) *AIChE J.* **2**, 420.
van Krevelen, D. W. and Hoftijzer, P. J. (1950) *Chem. Eng. Prog.* **46**, 29.
Wacholder, E. and Sather, N. F. (1974) *J. Fluid Mech.* **65**, 417.
Wairegi, T. and Grace, J. R. (1976) *Int. J. Multiphase Flow* **3**, 67.
Walters, J. K. and Davidson, J. F. (1962) *J. Fluid Mech.* **12**, 408.
Weber, M. E. and Bhaga, D. (1982) *Chem. Eng. Sci.* **37**, 113.
Wegener, P. P. and Parlange, J-Y. (1973) *Ann. Rev. Fluid. Mech.* **5**, 79.